This is a repository copy of *Evolution of complex flowering strategies: an age- and size-structured integral projection model* .

White Rose Research Online URL for this paper:
http://eprints.whiterose.ac.uk/1394/

Evolution of complex flowering strategies: an age- and size-structured integral projection model

Dylan Z. Childs[1], Mark Rees[1*], Karen E. Rose[1], Peter J. Grubb[2] and Stephen P. Ellner[3]

[1]*Department of Biological Sciences and NERC Centre for Population Biology, Imperial College, Silwood Park, Ascot SL5 7PY, UK*

[2]*Department of Plant Sciences, University of Cambridge, Cambridge CB2 3EA, UK*

[3]*Department of Ecology and Evolutionary Biology, Corson Hall, Cornell University, Ithaca, NY 14853-2701, USA*

We explore the evolution of delayed age- and size-dependent flowering in the monocarpic perennial *Carlina vulgaris*, by extending the recently developed integral projection approach to include demographic rates that depend on size *and* age. The parameterized model has excellent descriptive properties both in terms of the population size and in terms of the distributions of sizes within each age class. In *Carlina* the probability of flowering depends on both plant size and age. We use the parameterized model to predict this relationship, using the evolutionarily stable strategy (ESS) approach. Despite accurately predicting the mean size of flowering individuals, the model predicts a step-function relationship between the probability of flowering and plant size, which has no age component. When the variance of the flowering-threshold distribution is constrained to the observed value, the ESS flowering function contains an age component, but underpredicts the mean flowering size. An analytical approximation is used to explore the effect of variation in the flowering strategy on the ESS predictions. Elasticity analysis is used to partition the age-specific contributions to the finite rate of increase (λ) of the survival–growth and fecundity components of the model. We calculate the adaptive landscape that defines the ESS and generate a fitness landscape for invading phenotypes in the presence of the observed flowering strategy. The implications of these results for the patterns of genetic diversity in the flowering strategy and for testing evolutionary models are discussed. Results proving the existence of a dominant eigenvalue and its associated eigenvectors in general size- and age-dependent integral projection models are presented.

Keywords: delayed reproduction; structured model; adaptive landscape

1. INTRODUCTION

Reproductive delays are a ubiquitous feature of plant and animal life cycles, and explaining why organisms defer reproduction is a classic problem in evolutionary biology (Cole 1954). The main benefits of early reproduction accrue through reductions in mortality and generation time (Cole 1954; Bell 1980). In general, reductions in mortality increase fitness, whereas reductions in generation time increase fitness only under certain circumstances, and may have no effect on fitness in a density-regulated population (Mylius & Diekmann 1995). The costs of early reproduction are reduced fecundity and/or quality of offspring (Bell 1980).

In plants, the study of reproductive delays is complicated because plants vary continuously in size and there is enormous variation in growth between individuals. This means that the standard models, which assume growth is deterministic, perform poorly when applied to plants (Rees *et al.* 1999, 2000). To overcome these problems, previous studies have used analytical approximations, dynamic-state variable models or computationally expensive individual-based models (Kachi & Hirose 1985; de Jong *et al.* 1989; Wesselingh *et al.* 1997; Rees *et al.* 1999, 2000; Rose *et al.* 2002). Clearly, a mathematical frame-

work that allows (i) individuals to vary continuously in size and (ii) variation in growth is required. Integral projection models allow both these essential features of plant populations to be modelled in an elegant framework, which is easily parameterized using standard demographic data. When combined with methods for calculating measures of population growth, such as the net reproductive rate (R_0) and the finite rate of increase (λ), and ideas from evolutionary demography, this approach provides a powerful set of tools for exploring reproductive decisions in biologically realistic models (Cochran & Ellner 1992; Mylius & Diekmann 1995; Caswell 2001).

The integral projection model was introduced by Easterling *et al.* (2000) and subsequently developed for use in studying monocarpic plants by Rees & Rose (2002). The model eliminates the need to divide data into discrete classes, without requiring any extra biological assumptions (Easterling *et al.* 2000). Integral projection models have many properties in common with matrix models; for example, they allow the calculation of the stable size distribution, the population growth rate λ, and the sensitivities and elasticities of λ.

Integral projection models are appropriate for continuously size-structured populations. However, in many plant populations demographic rates are influenced by both size and age (Werner 1975; Gross 1981; van Groenendael & Slim 1988; McGraw 1989; Lei 1999; Karlsson & Jacobson 2001). In several monocarpic species, where long-term

datasets are available, the probability of flowering is determined by a plant's size *and* age (Klinkhamer *et al.* 1987; Rees *et al.* 1999; Rose *et al.* 2002). This is particularly puzzling in species such as *Carlina vulgaris* where all other demographic transitions are independent of plant age (Rose *et al.* 2002). Under these circumstances, the pay-off from flowering does not change as plants grow older and so the probability of flowering should not be influenced by plant age. Rose *et al.* (2002) suggest that under these circumstances age-dependent flowering might evolve because of temporal variation in mortality, because the population is part of a metapopulation or as a way of fine-tuning the flowering strategy. Additionally Rees *et al.* (2000) show, using a dynamic-state variable approach, that, when there is a finite time horizon (a maximum age), resulting from successional change or senescence, then there are fewer opportunities for growth as plants get older, and this selects for smaller sizes at flowering in old plants.

We present an extension to the integral projection approach allowing demographic transitions to depend on a plant's size *and* age. We first outline the construction of integral projection models for monocarpic plants with size-dependent and age-dependent demographic rates, and numerical methods for analysing them. The results of Easterling (1998), proving the existence of a dominant eigenvalue and associated eigenvectors, are then extended to cover general size- and age-dependent integral projection models. We then summarize the size- and age-dependent demography of *C. vulgaris* and use this to construct a size- and age-structured integral projection model. Using methods from evolutionary demography, we analyse the models to determine the evolutionarily stable flowering strategy under a variety of constraints (Mylius & Diekmann 1995).

2. MATERIAL AND METHODS

The integral projection model can be used to describe how a continuously size-structured population changes over discrete time (Easterling *et al.* 2000). The state of the population is described by a probability density function, $n(x,t)$, which can intuitively be thought of as the proportion of individuals of size x at time t. The integral projection model for the proportion of individuals of size y at time $t + 1$, 1 year later, is then given by

$$n(y,t + 1) = \int_{\Omega} [p(x,y) + f(x,y)]n(x,t)\mathrm{d}x$$
$$= \int_{\Omega} k(y,x)n(x,t)\mathrm{d}x. \quad (2.1)$$

where $k(y,x)$, known as the kernel, describes all possible transitions from size x to size y, including births. The integration is over the set of all possible sizes, Ω. The kernel is composed of two parts, a fecundity function, $f(x,y)$, and a survival–growth function, $p(x,y)$. To extend the model to include size- and age-dependent demography we define $n_a(y,t)$ to be the probability density function for individuals of size y and age a in year t. The integral projection model then becomes

$$n_0(y,t + 1) = \sum_{a=0}^{m} \int_{\Omega} f_a(x,y)n_a(x,t)\mathrm{d}x \qquad a = 0,$$
$$\qquad\qquad\qquad\qquad\qquad\qquad\qquad\qquad (2.2)$$
$$n_a(y,t + 1) = \int_{\Omega} p_{a-1}(x,y)n_{a-1}(x,t)\mathrm{d}x \qquad a > 0,$$

where $f_a(x,y)$ is the fecundity function, $p_a(x,y)$ is the survival–growth function of plants of size x and age a, and m is the maximum plant age. These functions are referred to collectively as the kernel component functions. For a numerical solution, it is convenient to write the model in matrix form, which is given by

$$\boldsymbol{n}(y,t + 1) = \int_{\Omega} \boldsymbol{K}\boldsymbol{n}(x,t)\mathrm{d}x, \quad (2.3)$$

where $\boldsymbol{K}$ is the matrix

$$\boldsymbol{K} = \begin{pmatrix} f_0(x,y) & f_1(x,y) & \cdots & f_{m-1}(x,y) & f_m(x,y) \\ p_0(x,y) & 0 & & 0 & 0 \\ 0 & p_1(x,y) & & 0 & 0 \\ & & \ddots & & \\ 0 & 0 & & p_{m-1}(x,y) & 0 \end{pmatrix} \quad (2.4)$$

and $\boldsymbol{n}(y,t) = (n_0(y,t),n_1(y,t),...,n_m(y,t))^T$. To solve these models we use numerical integration methods (Easterling *et al.* 2000). If each component function is evaluated at q equally spaced quadrature mesh points, y_i, and w is the quadrature weight (difference between the y_is), we can then approximate equation (2.3) as

$$\boldsymbol{n}(t + 1) = \tilde{\boldsymbol{K}}\boldsymbol{D}\boldsymbol{n}(\mathrm{t}), \quad (2.5)$$

where $\boldsymbol{n}(t) = (n_0(y_0,t),...,n_0(y_q,t),...,n_m(y_0,t),...,n_m(y_q,t))^T$,

$$\tilde{\boldsymbol{K}} = \begin{pmatrix} f_0(y_i,y_j) & f_1(y_i,y_j) & \cdots & f_{m-1}(y_i,y_j) & f_m(y_i,y_j) \\ p_0(y_i,y_j) & 0 & & 0 & 0 \\ 0 & p_1(y_i,y_j) & & 0 & 0 \\ & & \ddots & & \\ 0 & 0 & & p_{m-1}(y_i,y_j) & 0 \end{pmatrix} \quad (2.6)$$

and $\boldsymbol{D} = \mathrm{diag}(w)$. The $\tilde{\boldsymbol{K}}\boldsymbol{D}$ matrix has the same form as Goodman's transition matrix, the properties of which have been carefully analysed (Goodman 1969; Law 1983). In Appendix A we prove that, under biologically reasonable assumptions, the model (equation (2.2)) has a dominant eigenvalue, λ, that is positive and strictly exceeds all others, and, when growing at a constant rate, λ, the population settles to a stable size–age distribution, which is given by the right-hand dominant eigenvector.

To calculate R_0, which is required for the evolutionary calculations, the general methods described in Caswell (2001) can be used. However, a considerable saving in computer time and memory can be achieved by collapsing the $\tilde{\boldsymbol{K}}\boldsymbol{D}$ matrix to a Leslie matrix. The key assumption required to collapse the $\tilde{\boldsymbol{K}}\boldsymbol{D}$ matrix is that the probability distribution of offspring sizes is independent of adult size and age (Law & Edley 1990; see Appendix A). We can then construct a Leslie matrix, the eigenvalues of which are equal to those of $\tilde{\boldsymbol{K}}\boldsymbol{D}$, and calculate R_0 using the standard age-based formula.

To apply the model we must specify the dependence of survival, growth and fecundity on size and age. We will present the equations for *C. vulgaris*, which has only size- *and* age-dependent flowering, but it is straightforward to extend the approach to include size and age dependence of other demographic transitions. Specifically, we will write the fecundity function as

$$f_a(x,y) = p_e s(x) p_{f,a}(x)f_n(x)f_d(x,y), \quad (2.7)$$

where p_e is the probability of seedling establishment, $s(x)$ is the

probability of survival of an individual of size x, $p_{f,a}(x)$ is the probability that an individual of size x and age a flowers, $f_n(x)$ is the number of seeds produced, and $f_d(x,y)$ is the probability distribution of offspring size, y, for an individual of size x. The survival–growth function is given by

$$p_a(x,y) = s(x)[1 - p_{f,a}(x)]g(x,y), \tag{2.8}$$

where $g(x,y)$ is the probability of an individual of size x growing to size y. The probability of flowering, $p_{f,a}(x)$, enters the survival function because reproduction is fatal in monocarpic species.

To compare the model predictions with field data, we calculate the stable flowering-size distribution, $\varpi(y)$, using

$$\varpi(y) = \frac{\sum_{a=0}^{m} s(y)p_{f,a}(y)\omega_a(y)}{\sum_{a=0}^{m} \int_{\Omega} s(y)p_{f,a}(y)\omega_a(y)\mathrm{d}y}, \tag{2.9}$$

where $\omega_a(y)$ is the stable size–age distribution.

(a) *Population biology of C. vulgaris*

Carlina vulgaris, a monocarpic thistle of base-rich soils (mainly found on limestone or calcareous sand), is native to a wide area in western, central and eastern Europe, and has been introduced to North America and New Zealand. Under very favourable growing conditions, *Carlina* individuals can flower in their second year (Klinkhamer *et al.* 1991, 1996; Rees *et al.* 2000) but, more commonly, reproduction is delayed by at least one more year. Previous studies in The Netherlands (Klinkhamer *et al.* 1991, 1996) have shown that the probability of flowering is related to plant size and not to age; however, in the UK the probability of flowering is related to both plant size and age (Rose *et al.* 2002). Flowering occurs between June and August, and the seeds are retained in the flower heads until they are dispersed during dry sunny days in late autumn, winter or spring (P. J. Grubb, unpublished data). Seeds germinate from April to June, and there is little evidence of a persistent seed bank (Eriksson & Eriksson 1997; de Jong *et al.* 2000).

Detailed descriptions of the study site and methods of analysis are given in Rose *et al.* (2002). We briefly describe the main results that are relevant to this article. The study spanned 16 years, and during this time the fates of over 1400 individuals were followed. The length of the longest leaf was used to measure plant size and in all analyses this was transformed using natural logarithms. Growth was strongly size-dependent and well described by a simple linear model:

$$L(t + 1) = a_g + b_g L(t). \tag{2.10}$$

Size this year predicted size next year ($F_{1,507} = 667.52$, $p < 0.0001$), but there was no significant effect of age ($F_{1,507} = 0.32$, $p = 0.576$); the parameter values were $a_g = 1.21$ (0.09) and $b_g = 0.71$ (0.03), where the standard error is given in parentheses. Generalized linear models of the probabilities of mortality and flowering were constructed assuming binomial errors and a logit link function (McCullagh & Nelder 1989). There was no effect on survival probability of plant size ($\chi_1^2 = 0.98$, $p > 0.30$) or age ($\chi_1^2 = 2.31$, $p > 0.10$); the parameter value was $\mathrm{logit}(s(x)) = 0.34$ (0.06). Plant size was the most important predictor of flowering ($\chi_1^2 = 139.86$, $p < 0.0001$), with larger plants being more likely to flower than smaller ones. There was an additional effect of age ($\chi_1^2 = 19.37$, $p < 0.001$), such that older plants were more likely to flower. The age effect was still significant ($p < 0.001$) after fitting year effects and

Table 1. Field data and model predictions.
(Values in parentheses are 95% confidence intervals.)

	data	model
average number of plants	74.4 (47.9, 101)	81.7
average size (mm)	32.8 (31.5, 34.1)	31.1
average age (years)	0.84–0.94	0.92
average size at flowering (mm)	52.0 (48.4, 55.6)	52.0
average age at flowering (years)	3.1 (2.7, 3.4)	2.8

allowing the size effect to be a smoothed function (generalized active model; Wood 2001). In the fitted logistic model for flowering, we will refer to the intercept, size slope and age slope as β_0, β_s and β_a, respectively; parameter values are given in table 2. To understand what the logistic regression means biologically it is necessary to distinguish between the threshold size for flowering, i.e. the size a plant must exceed in order to initiate flowering, and the size at flowering. These are different because (i) plants that flower are larger than the threshold size for flowering and (ii) there is variable growth between the time the decision to flower is made and the time at which flowering is recorded. However, we may interpret the fitted logistic model as a cumulative distribution function describing the threshold sizes for flowering. This implies that the probability density function of threshold sizes for flowering for plants of age a is described by a logistic distribution with mean and variance of $-(\beta_0 + a\beta_a)/\beta_s$ and $\pi^2/3\beta_s^2$, respectively (Rees & Rose 2002). The mean size of flowering individuals observed in a population is obtained using equation (2.9). There was no relationship between this year's seed production and the number of recruits in the following year, suggesting that the probability of recruitment is density dependent (Rose *et al.* 2002); the mean number of recruits was 39.8 per year. This decoupling of recruitment from seed production was probably the result of establishment being limited by the available microsites: more seedlings are recruited when the turf was either short or opened up locally by trampling cattle (P. J. Grubb, personal observation). Two seed-sowing experiments, one in Sweden and one in Wales, support the idea that recruitment is dependent on disturbance (Greig-Smith & Sagar 1981; Lofgren *et al.* 2000). Thus, if there are R recruits into the population, the probability of establishment is given by

$$p_e = \frac{R}{\sum_{a=0}^{m} \int_{\Omega} \int_{\Omega} f_a(x,y)n_a(x,t)\mathrm{d}x\mathrm{d}y}. \tag{2.11}$$

Data were not available on the sizes of recruits derived from plants of different sizes, but evidence from other systems suggests a low maternal effect on recruit size (Weiner *et al.* 1997; Sletvold 2002), and so the distribution of offspring sizes was assumed to be independent of parental size; the parameter values were mean = 3.09, variance = 0.28—logarithmic scale.

3. RESULTS

(a) *Analysis of the kernel*

Having produced a parameterized model, we can assess the model's descriptive properties by calculating the stable size–age distribution and comparing this with the observed data. This shows that there is good agreement between the model and the observed size–age distribution (figure 1).

Table 2. Evolutionarily stable flowering strategy in terms of the parameters of the flowering function and the average size and age at flowering, assuming either that there are no constraints or that the slope of the flowering function, β_s, is constrained at its estimated value.

(For reference the estimated values are also given; values in parentheses are 95% confidence intervals.)

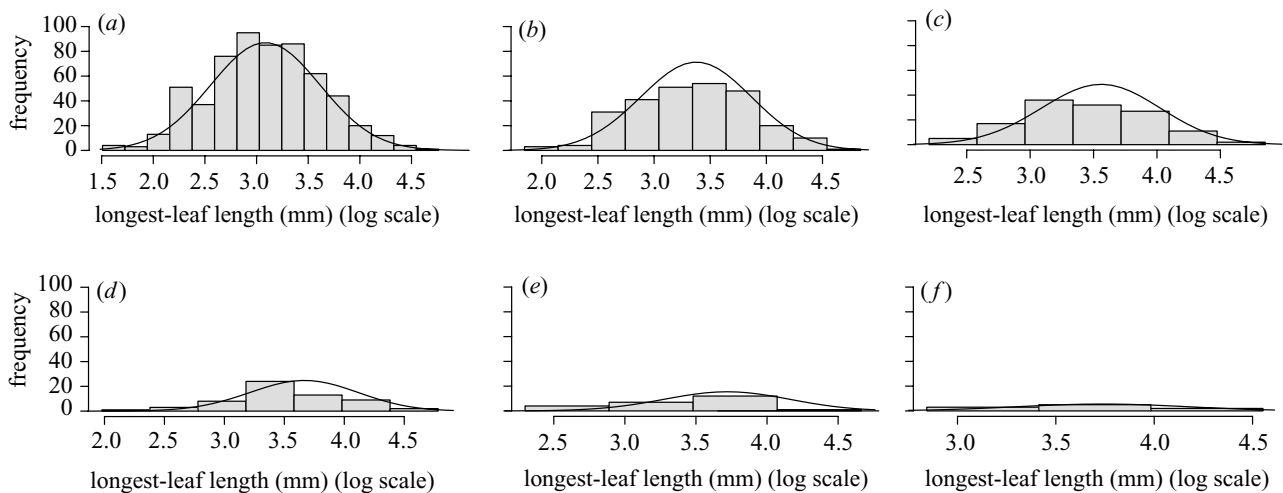| | parameter | | | predicted values | |
	β_0	β_s	β_a	size at flowering (mm)	age at flowering (years)
unconstrained ESS	−1010	278	0.01	50.1	2.1
constrained ESS	−9.96	—	0.38	37.9	1.7
estimated value	−12.05 (−9.84, −14.26)	2.64 (2.06, 3.22)	0.32 (0.18, 0.45)	52.0 (48.4, 55.6)	3.1 (2.7, 3.4)

Figure 1. Observed (filled bars) and predicted (lines) stable size–age distributions for ages 0–5 years, (a)–(f), respectively. The bar width in each histogram was chosen using a kernel density estimation routine to make the plots maximally informative.

We also calculated various measures of population size and age structure, using the methods outlined in Rees & Rose (2002) and, in all cases, the model predictions were in excellent agreement with the field data (table 1). As density dependence is explicitly modelled, we can calculate the equilibrium population size, and again there is excellent agreement between the model and the data (table 1).

(b) Evolution of the flowering strategy

To calculate the evolutionarily stable flowering strategy we need to specify not only how demographic rates vary with size and age but also where in the life cycle density dependence acts (Mylius & Diekmann 1995). In *Carlina*, the probability of seedling establishment is density dependent, while the effect of intraspecific competition is weak (Rose *et al.* 2002). Under these conditions it can be shown that the evolutionarily stable strategy (ESS) maximizes the basic reproductive rate, R_0 (Mylius & Diekmann 1995; Rees & Rose 2002). We used a quasi-Newton algorithm to maximize R_0 and so characterize the ESS. Given the evolutionarily stable flowering strategy we then use equation (2.9) to calculate the distribution of sizes at flowering.

Allowing all three parameters to vary, we find that the ESS tends towards a step function without an age component (table 2). Specifically, the variance of the flowering-threshold distribution tends to zero as $\beta_s \rightarrow \infty$ and $\beta_a \rightarrow 0$. This matches our expectations for a constant-environment model in which the key demographic processes of growth, survival and fecundity are all independent of age. The flowering-size threshold in this case (given by $\exp(-\beta_0/\beta_s)$) tends to 37.8 mm, and the predicted average size at flowering is not significantly different from the observed value (table 2). However, the variance in the distribution of flowering sizes is much smaller than that observed in the data (figure 2).

We also calculated the ESS assuming that the size-dependent slope of the flowering function, β_s, was fixed. We use this constraint to prevent the ESS from being a step function. There are several reasons why it might be impossible for plants to achieve a step function: (i) there is variable growth between when the decision to flower is made and when plant size is measured; (ii) plant size may not be perfectly correlated with the threshold condition for flowering; and (iii) there may be genetic variation in the threshold condition. With β_s constrained the predicted flowering strategy (β_0, β_a) is similar to the observed strategy, although the predicted size at flowering is considerably smaller than that observed in the field (table 2). As expected, because β_s is fixed, the variance in the size at flowering is similar to that observed in the field (figure 2). Interestingly, when we constrain β_s, the predicted flowering strategy is both size-specific and age-specific.
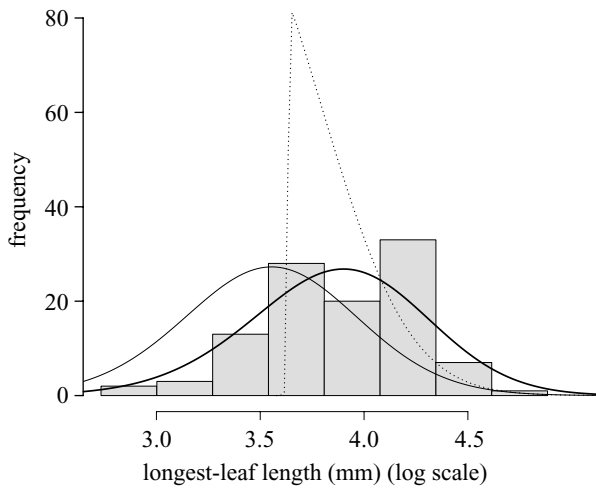
Figure 2. Observed distribution of flowering sizes (filled bars) and predictions from the various models, calculated using equation (2.9). The bold line is the fitted model, the dotted line is from the unconstrained ESS model and the solid thin line is from the constrained ESS model.

(c) Analytical approximation

To understand how different aspects of *Carlina*'s demography influence the observed flowering size we extend the 1-year look-ahead approach described in Rees *et al.* (2000). The approach derives a switch value L_s: on average, plants with $L(t) > L_s$ are expected to flower, while plants with $L(t) < L_s$ are expected to continue growing. The switch value is determined by equating expected seed production given the current size, L_s, with expected seed production in the following year, taking growth and mortality into account. It should be noted that the approach is only approximate because it ignores opportunities for growth more than 1 year ahead. In this system, the probability of survival is independent of size and age such that the survival function can be written as

$$s(x) = \exp(-d_0). \tag{3.1}$$

Growth is described by equation (2.10) and seed production is given by

$$\text{seed production} = \exp(A + BL(t)). \tag{3.2}$$

Placing the component functions together we find that the switch value, L_s, satisfies the equation

$$\int \exp(A + B(L_s + \varepsilon_f)) f(\varepsilon_f) \mathrm{d}\varepsilon_f$$

$$= \iint \exp(-d_0 + A + B(a_g + b_g(L_s + \varepsilon_f)) + \varepsilon) f(\varepsilon_f) f(\varepsilon) \mathrm{d}\varepsilon_f \mathrm{d}\varepsilon, \tag{3.3}$$

where $f(\cdot)$ is the normal probability density function, ε_f describes the between-individual variation in L_s, and ε describes the variation around the growth function. Evaluating the integrals and solving for L_s we find

$$L_s = \frac{a_g + B\sigma^2/2}{(1 - b_g)} - \frac{d_0}{B(1 - b_g)} - \frac{\sigma_f^2 B(1 - b_g)}{2}, \tag{3.4}$$

where σ^2 is the variance about the growth equation (2.10). The first and second terms describe the effects of growth and mortality, respectively, on the mean switch size. The

first term is related to the arithmetic asymptotic average size; this is given by

$$l = \frac{a_g + \sigma^2/2}{1 - b_g}. \tag{3.5}$$

As expected, the switch value increases with increasing asymptotic size and decreases with increasing mortality. The dependence of the mean switch value, L_s, on variation in the switching size is less intuitive: increasing variability around the mean switch size selects for smaller switch sizes, because the variance term, σ_f^2, which arises because of nonlinear averaging, is always negative. There was excellent agreement between the unconstrained ESS flowering threshold size (37.8 mm), for which $\sigma_f^2 = 0$, and the predicted switch value, 36.7 mm, calculated using equation (3.4). The 1 year look-ahead approach predicts a lower switch value because it ignores growth more than 1 year ahead; however, the discrepancy is small because of high size-independent mortality. Comparison of the two approaches in the constrained case is complicated because the ESS contains an age component. However, the 1 year look-ahead approach correctly predicts that variance in the threshold condition selects for smaller flowering sizes.

(d) Fitness and adaptive landscapes

In this system density dependence acts on the recruitment stage and so evolution maximizes R_0. A plot of R_0 against the flowering strategy can be interpreted as an 'adaptive landscape' in the classical sense (Wright 1931). Its topography is unaltered by the presence of a particular resident, and an ESS is defined by a local maximum. At equilibrium $R_0 = \lambda = 1$ and so λ represents the rate of invasion of new strategies into the resident population, such that the surface for λ represents a fitness landscape. Its topography describes the strengths of selection acting on alternative strategies (Metz *et al.* 1992; Rand *et al.* 1994). We computed the adaptive and fitness landscapes for a wide range of β_0 and β_a, assuming β_s was fixed (figure 3). When interpreting these graphs it must be remembered that as β_0 gets smaller (more negative) so the size at flowering increases. The adaptive landscape shows that the ESS lies within the 95% confidence envelope for the estimated parameters. Moving from left to right across the adaptive landscape we see a dramatic increase in the performance of the flowering strategy; this reaches a maximum then declines to a plateau where all strategies have equal R_0. Clearly, flowering at sizes much larger than the ESS results in a dramatic loss of fitness. This is a consequence of high size-independent mortality (*ca.* 40% of plants die each year). The plateau in the adaptive landscape, corresponding to large values of β_0, occurs because all plants flower in their first year, and so have equal performance (R_0). Moving vertically across the adaptive landscape, we see much smaller changes in performance (figure 3a). This is a direct result of growth and seed production being determined by plant size rather than age. The fitness landscape demonstrates that there would be strong selection towards the ESS, as the fitness difference between the estimated ESS and the predicted ESS is *ca.* 10% (figure 3b). In the vicinity of the estimated ESS there is very weak selection for an age-dependent component to the flowering strategy.
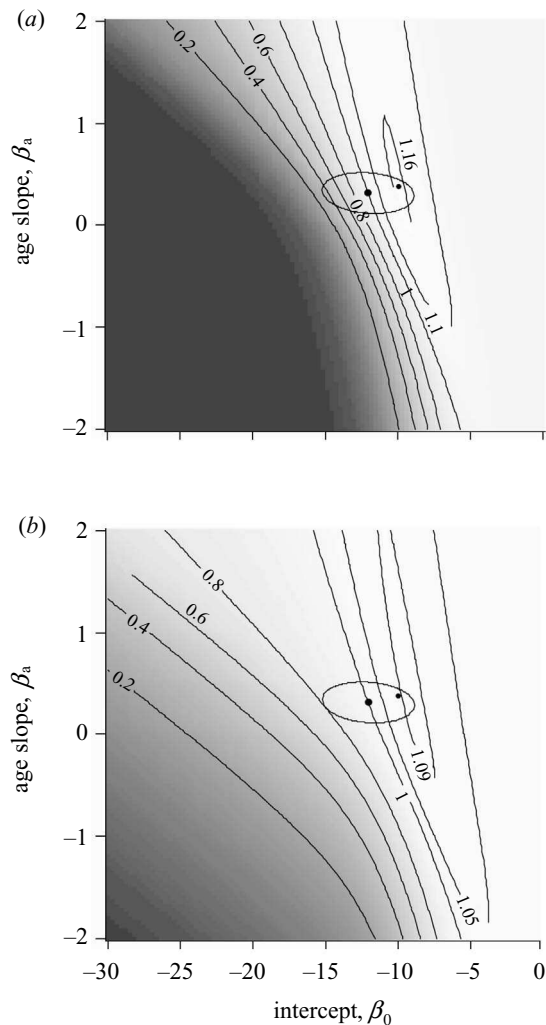
Figure 3. The (a) adaptive and (b) fitness landscapes for *Carlina*, calculated assuming that the resident population uses the estimated flowering strategy. The large dot is the estimated flowering strategy, and the ellipse is the 95% confidence contour, calculated using the standard quadratic approximation to the likelihood—assuming that the likelihood is χ^2-distributed with three degrees of freedom. The small dot is the ESS prediction assuming β_s is fixed.

(e) *Sensitivities and elasticities*

The standard approach for understanding how various parameters influence the fitness of rare mutants is to estimate the elasticities of mutant fitness (Caswell 2001). Elasticities can be used to measure the effect on λ of proportional changes in $f_a(x,y)$ and $p_a(x,y)$ and can be computed using the methods described in Easterling *et al.* (2000) (see Appendix A). As elasticities sum to unity, this allows us to partition the contributions of $f_a(x,y)$ and $p_a(x,y)$ to λ of different age classes (figure 4a,b). This shows that the survival–growth function has a larger influence on λ than does the fecundity function (0.66 and 0.34, respectively), and that the largest contributions to λ come from changes in the survival–growth function, $p_a(x,y)$, of young plants.

4. DISCUSSION

We have extended the integral projection modelling approach to include a discrete structuring variable such as age, allowing us to explore the demography and evolution of size- and age-structured populations using a set of standard numerical techniques. The analytical results (Appendix A) justify the numerical methods used and should prove useful in future studies where the distribution of offspring sizes depends on parental size or age. The 'mixing at birth' assumption is likely to be valid for a wide range of species, particularly when the size distribution of recruits is recorded several months after recruitment occurs (Weiner *et al.* 1997; Sletvold 2002). In contrast to age- and size-structured matrix models, where parameterization is difficult (Law 1983), extending an integral projection model to include the effects of age can be done by including age as an additional covariate when constructing the survivorship, growth or flowering functions. This means that a standard statistical test can be used to explore whether both size and age should be included in the model (Venables & Ripley 1997). Hence, this framework retains all of the power of traditional matrix models while being easy to parameterize.

The parameterized model provides an extremely accurate description of the number of individuals and the distribution of sizes within each age class, the distribution of flowering sizes, the average age at reproduction and the average population size. Despite this, the ESS predictions differ in either the mean or the variance from the observed distribution of flowering sizes. These discrepancies force us to conclude that important aspects of the selection pressures acting on *Carlina* are not included in the model. The analyses presented by Rose *et al.* (2002) strongly suggest that temporal variation in demographic rates is a missing component of the selective environment. In this study, temporal variation in the intercept of the survival and growth functions was found to select for larger sizes at flowering. Curiously, the parameters of the constrained ESS are not significantly different from the estimated parameters of the flowering function, which suggests that one needs to be careful when comparing the predictions of evolutionary models with data, as different metrics may produce different results. Clearly, any satisfactory model needs to describe both the shape of the flowering function and the distribution of sizes at flowering, and we cannot assume that a model that is correct in one respect will be correct in the other.

Why does the flowering function contain an age-dependent term when the key demographic processes of growth and survival are independent of age? First, it must be acknowledged that the apparent age dependence could be an artefact of using an indirect measure of plant size, namely the length of the longest leaf. If older plants have larger tap roots for a given longest-leaf length, then the resources available for flowering to an older plant will be underestimated, resulting in an apparent increase in the probability of flowering with age. We know of no data on age-dependent resource allocation and therefore cannot discount this possibility, although Klinkhamer *et al.* (1987) found that longest-leaf length was the best predictor of total plant weight in *Cirsium vulgare*, a monocarpic plant that also has size- and age-dependent flowering.

Allowing all three parameters to evolve results in an age-independent flowering strategy, where the relationship between the probability of flowering and size is a step function, as expected. When we constrain the ESS so that
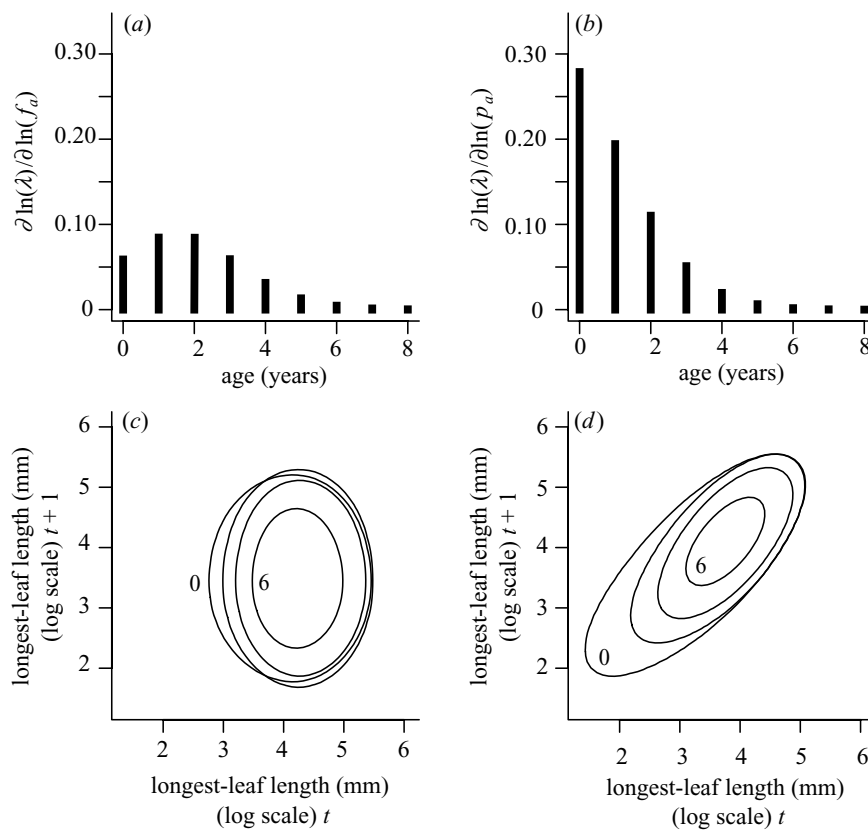
Figure 4. Elasticity analysis for the kernel component functions. Elasticity values are summed over size for (a) $f_a(x,y)$ and (b) $p_a(x,y)$ for all age classes. Elasticity contour plots for (c) $f_a(x,y)$ and (d) $p_a(x,y)$ for age classes 0, 2, 4 and 6 years. Contour plots show the 0.000 003 contour for each age class.

the flowering strategy cannot be a step function, the model predicts that the ESS has an age-dependent component. This conforms to the 'fine-tuning' hypothesis put forward by Rose *et al.* (2002): this hypothesis argues that having two control variables (e.g. size and age) is advantageous as it allows extra control of the flowering strategy. However, the fitness of the age-dependent constrained ESS when invading a resident strategy employing a purely size-dependent constrained ESS is only 1.0010. Therefore, there is very weak selection for age dependence via the 'fine-tuning' hypothesis and so this mechanism is unlikely to be responsible for age dependence in *Carlina*. However, a wide range of age-dependent strategies ($0.0 < \beta_a < 0.95$) are marginally fitter ($1.000 \leq \lambda \leq 1.001$) than the purely size-dependent constrained ESS, suggesting that age dependence is an approximately neutral trait. This is consistent with the observation that in Dutch populations of *Carlina* (Klinkhamer *et al.* 1991, 1996) the probability of flowering is not related to plant age.

Age-dependent flowering could arise if there is variation in the probability of flowering at a given size. Imagine a population consisting of equal numbers of two flowering strategies, one with a small threshold for flowering and the other with a large threshold. As the cohort ages the plants with the small thresholds flower earlier, leaving a cohort with large thresholds that flower later. In this scenario the probability of flowering would be age dependent, although we would observe an increase in the size threshold for flowering with age, the opposite of what is seen in *Carlina* (see Rees & Long (1993) for a general discussion of this phenomenon). Similar effects would occur if growth or

mortality varied consistently between individuals. No evidence for consistent variation between individuals in growth, flowering or survival was found in *Carlina* using mixed models (Rose *et al.* 2002), making this explanation unlikely.

When constraining β_s to the observed value we are assuming that the variance in the flowering strategy is not subject to selection. This seems reasonable providing that the decision to flower is made some months before plant size at flowering is recorded, growth during this period is highly variable and there is little genetic variation in the threshold size for flowering. The exact time the decision to flower is made is not known in *Carlina* (Klinkhamer *et al.* 1991); however, growth is highly variable suggesting that the observed graded relationship between size and the probability of flowering reflects, in part, variation in growth between the time the decision to flower is made and the time at which the size is recorded. In addition to this, the control of flowering in *Carlina* depends on a complex interaction between exposure to cold, day length and size before and after winter (Klinkhamer *et al.* 1991). This means that size will not be perfectly correlated with the threshold condition for flowering and this too will tend to make the relationship between the probability of flowering and plant size shallower. However, it should be noted that several studies have demonstrated that natural populations harbour genetic variation in the threshold size for flowering (Metcalf *et al.* 2003; Wesselingh & de Jong 1995; Wesselingh & Klinkhamer 1996; Simons & Johnston 2000), which will be subject to selection, and this could lead to an increase in β_s.

Elasticity analysis has been used to partition contributions to λ from different kernel component functions, age classes and sizes. Care must be taken when interpreting elasticity patterns because the fecundity and survival–growth functions both contain survival and probability-of-flowering terms. In this system the survival–growth functions make a greater contribution to λ than do the fecundity functions, because reductions in growth and survival of a particular age class lessen the opportunities for reproduction in subsequent years. In general, younger plants contribute most to λ because they represent a larger proportion of the stable age distribution (figure 4*a,b*). However, this underlying trend is tempered by the fact that younger, and hence smaller, plants contribute relatively few recruits to the next generation. Elasticity contour plots for the fecundity functions demonstrate that contributions to λ through recruitment are most important for large individuals, while λ is influenced by the survival of a wide range of sizes (figure 4*c,d*). Individuals are, on average, larger as they grow older, and this is reflected by a shift in the high-density regions of the elasticity surfaces towards larger sizes for older age classes. The technique for partitioning elasticities into age- and size-dependent components can also be used for populations with purely size-dependent demography.

The shapes of the adaptive and fitness landscapes have important implications for: (i) the patterns of genetic variation in threshold sizes for flowering found in natural populations; and (ii) testing evolutionary models. In a study of two monocarpic species by de Jong *et al.* (1989), fitness increased rapidly with plant size, reached a maximum, then very slowly declined for large threshold sizes for flowering—in contrast to what we see for *Carlina*. This means that a wide range of flowering strategies are consistent with de Jong *et al.*'s model, and allowance must be made for this when testing evolutionary predictions of the model. Given de Jong *et al.*'s fitness landscape we would predict that the distribution of flowering thresholds would be highly asymmetric with a long tail to the right (i.e. a wide range of plants would have flowering thresholds larger than the optimum or ESS prediction). One possible explanation for the difference between these studies is that in de Jong *et al.* (1989) large plants had high survival (greater than 80%) and so the fitness penalties of having a large threshold size for flowering were relatively small. Understanding how systematic variation in demographic rates with age and size influences fitness landscapes is clearly an area that warrants further study. The hybrid matrix–integral projection model should contribute to these studies by facilitating the precise quantitative assessment of a broad range of life-history strategies.

APPENDIX A: DYNAMICS OF THE AGE–SIZE INTEGRAL PROJECTION MODEL

(a) *The* C. vulgaris *model*

The age–size integral projection model for *C. vulgaris* has some special features that allow an elementary analysis based on Leslie matrix theory: (i) all living individuals have some probability of reproducing now or later; and (ii) the size distribution of new offspring (age = 0) is the same for all parents:

$$f_d(x,y) = \varphi_0(y), \tag{A 1}$$

where φ_0 is the probability distribution of offspring size for all parents. Thus, as with its numerical approximation by the $\tilde{K}D$ matrix, the forward dynamics of the model itself can be reduced to those of a Leslie matrix model. For the sake of future age–size models in which equation (A 1) will often not be true, we indicate in the second section of this appendix how the assumptions implicit in equation (A 1) can be relaxed without affecting the conclusions.

Assuming equation (A 1), after a possible initial transient of length m (the maximum age), all individuals of age $j > 0$ are descended from an offspring cohort with size distribution φ_0 and therefore have size distributions proportional to $\varphi_j(y)$, where

$$\psi_{j+1}(y) = \int_\Omega \varphi_j(x)\, p_j(x,y)\mathrm{d}x, \quad \varphi_{j+1} = \psi_{j+1} \Big/ \int_\Omega \psi_{j+1}. \tag{A 2}$$

The *per capita* fecundity of individuals of age j is then $F_j = \int_\Omega \int_\Omega \varphi_j(x) f_j(x,y)\mathrm{d}x\mathrm{d}y$ and the fraction surviving to age $j + 1$ is $P_j = \int_\Omega \int_\Omega \varphi_j(x)\, p_j(x,y)\mathrm{d}x\mathrm{d}y$. The state of the population at time t is specified by the vector of the total numbers in each age class, $N(t) = [N_0(t),N_1(t),\ldots,N_m(t)]$, which satisfies the Leslie matrix model,

$$N(t + 1) = \begin{vmatrix} F_0 & F_1 & \cdots & F_{m-1} & F_m \\ P_0 & 0 & \cdots & 0 & 0 \\ 0 & P_1 & \cdots & 0 & 0 \\ \vdots & \vdots & \ddots & \vdots & \vdots \\ 0 & 0 & \cdots & P_{m-1} & 0 \end{vmatrix} N(t). \tag{A 3}$$

This is a primitive Leslie matrix (as two successive Fs are positive), so it has a dominant eigenvalue giving the long-term growth rate $\lambda > 0$, and the population converges to the size distribution resulting from the corresponding eigenvector w, $n_j(x,t) \sim C\lambda^t w_j \varphi_j(x)$, where the constant C depends on the initial conditions. It is straightforward to verify that this distribution is an eigenvector of the integral model, with eigenvalue λ.

The derivation of the eigenvalue-sensitivity formula for the size-structured integral model (Easterling 1998) uses only the existence of the left and right eigenvectors corresponding to the dominant eigenvalue λ, and therefore carries over to the age–size model. The existence of a dominant left eigenvector is guaranteed by general operator theory (see § c below).

(b) *A more general age–size model*

In general, for an age–size model to have a unique long-term growth rate and a stable age–size distribution, it is not sufficient for the age-transition Leslie matrix (which has the form of equation (A 3)) to be primitive. First, as in a Leslie matrix, we need to eliminate individual types that have no chance of reproducing in the future, by building the model (and estimating the kernel) as if such individuals were already dead. Otherwise, an initial population could die out or grow depending on whether it consists entirely of post-reproductives. We therefore assume that for all age–size values x_j there exists a $q > 0$ and a newborn size y_0 such that $k_{0,j}^{(q)}(y_0,x_j) > 0$, where $k_{ij}^{(n)}$ denotes

the n-step-ahead transition kernel between ages j and i; note that $q \leqslant m$ (the maximum possible lifespan). For this assumption to hold, the size range Ω may need to be trimmed in an age-dependent manner, so we define Ω_j to be the range of possible sizes for an individual of age j. Typically, each Ω_j will be a closed interval, but nothing changes if each Ω_j is a finite union of closed intervals.

We also need some degree of 'mixing' in the size distribution, to rule out situations where small parents produce a small number of small offspring who grow up to be small parents with low fecundity, while large parents have a large number of large offspring, etc. In such cases, different initial conditions could result in different population growth rates. One simple possibility is *mixing at birth*: parent size affects the distribution of offspring size but not the range of possible sizes. Formally, in place of equation (A 1), assume that there exists a continuous non-negative function $\varphi_0(y)$ on Ω_0 and constants $c > 0$ and $C > 0$ such that all age-specific offspring-size distributions satisfy

$$c\varphi_0(y) \leqslant f_{\mathrm{d},a}(x,y) \leqslant C\varphi_0(y) \qquad \text{(A 4)}$$

for all age–size values x with non-zero present fecundity. Then, as in the *Carlina* model, we can define a Leslie matrix $\boldsymbol{L}_0$ by assigning the size distribution φ_0 to all offspring and computing their future prospects. Assume that $\boldsymbol{L}_0$ is primitive (irreducible and aperiodic). From these assumptions we can show that some iterate of the kernel is *u-bounded* (Krasnosel'skij *et al.* 1989), which implies the existence of a unique positive dominant eigenvalue and corresponding eigenvectors (see § c below). Convergence to a stable age–size distribution from generic initial conditions then follows from the spectral decomposition for compact operators, exactly as in Easterling (1998).

(c) *Details*
(i) *Transition operator*
To understand this section, one needs to know some functional analysis. A density-independent integral projection model defines a linear operator $\boldsymbol{T}$ on an appropriate function space of population-distribution functions—for the age–size model with continuous kernels this is the space $C(\boldsymbol{X})$ of continuous functions on the set $\boldsymbol{X}$ consisting of the m size ranges $\Omega_0, \Omega_1,\ldots,\Omega_m$ (each regarded as sitting in its own copy of the real line) with Lebesgue measure and topology inherited from the real line. The natural space of population distribution functions is $L_1(\boldsymbol{X})$, the space of age–size distributions with a finite total population, but as the kernel components are bounded and continuous it follows that $\boldsymbol{T}$ maps $L_1(\boldsymbol{X})$ into $C(\boldsymbol{X})$, so we can regard $\boldsymbol{T}$ as an operator on $C(\boldsymbol{X})$. $\boldsymbol{X}$ is a compact Hausdorff space and the kernel components are all continuous, so $\boldsymbol{T}$ is compact (Dunford & Schwartz 1988, p. 516). $\boldsymbol{T}$ clearly preserves the cone of non-negative continuous functions in $C(\boldsymbol{X})$, which is a reproducing cone (Krasnosel'skij *et al.* 1989, p. 9). Any iterate $\boldsymbol{T}^t$ will also have these last two properties.

(ii) *Left eigenvectors*
'Left eigenvector' in this context means an eigenvector of the adjoint operator $\boldsymbol{T}^*$. For any non-zero element in the spectrum of a compact operator (in particular, for the dominant eigenvalue), both the operator and its adjoint have corresponding eigenvectors (Dunford & Schwartz 1988, p. 578), as required.

(iii) u-Bounds
Upper and lower u-bounds under mixing-at-birth can be constructed as follows. Let $n(y,0) = n_0(y)$ be an initial size distribution in $C(\boldsymbol{X})$. By assumption, there exists a future time, q, which may depend on n_0, at which some births occur. Since $\boldsymbol{L}_0$ is primitive, there exists some time interval Q such that all entries in $\boldsymbol{L}_0^t$ are strictly positive for all $t \geqslant Q$. Hence, at time $M = m + Q$, the offspring of the individuals born at time q include individuals of all ages $j = 0,1,2,\ldots,m$. These individuals were necessarily born $0,1,2,\ldots,m$ time-steps previously. We can therefore define $N_{\min}(n_0), N_{\max}(n_0)$ as the minimum and maximum of the total numbers of offspring born in each of those years, with $N_{\min}(n_0) > 0$ and $N_{\max}(n_0)$ finite since the kernel is bounded. Using equation (A 4) to bracket the actual size distributions of offspring in those years, we then have

$$cN_{\min}u_0(y) \leqslant n(y,M) \leqslant CN_{\max}u_0(y), \qquad \text{(A 5)}$$

where $u_0 = (\boldsymbol{I} + \boldsymbol{T} + \boldsymbol{T}^2 + \ldots + \boldsymbol{T}^m)\varphi_0$.

This is exactly the definition of $\boldsymbol{T}^M$ being u_0-bounded. $\boldsymbol{T}^M$ therefore satisfies the assumptions of theorems 11.1(b) and 11.5 in Krasnosel'skij *et al.* (1989) and consequently has a unique dominant eigenvalue, which is positive and equal to its spectral radius, with all other points in the spectrum being strictly smaller in magnitude. The same is therefore also true for $\boldsymbol{T}$, as shown in the proof of theorem A4 in Easterling (1998).

REFERENCES

Bell, G. 1980 The costs of reproduction and their consequences. *Am. Nat.* **116**, 45–76.

Caswell, H. 2001 *Matrix population models. Construction, analysis and interpretation.* Sunderland, MA: Sinauer.

Cochran, M. E. & Ellner, S. 1992 Simple methods for calculating age-based life-history parameters for stage-structured populations. *Ecol. Monogr.* **62**, 345–364.

Cole, L. C. 1954 The population consequences of life history phenomena. *Q. Rev. Biol.* **29**, 103–137.

de Jong, T. J., Klinkhamer, P. G. L., Geritz, S. A. H. & van der Meijden, E. 1989 Why biennials delay flowering—an optimization model and field data on *Cirsium vulgare* and *Cynoglossum officinale*. *Acta Bot. Neerland.* **38**, 41–55.

de Jong, T. J., Klinkhamer, P. G. L. & de Heiden, J. L. H. 2000 The evolution of generation time in metapopulations of monocarpic perennial plants: some theoretical considerations and the example of the rare thistle *Carlina vulgaris*. *Evol. Ecol.* **14**, 213–231.

Dunford, N. & Schwartz, J. T. 1988 *Linear operators. Part I: general theory.* New York: Wiley.

Easterling, M. R. 1998 The integral projection model: theory, analysis and application. PhD thesis, North Carolina State University, Raleigh, NC, USA.

Easterling, M. R., Ellner, S. P. & Dixon, P. M. 2000 Size-specific sensitivity: applying a new structured population model. *Ecology* **81**, 694–708.

Eriksson, A. & Eriksson, O. 1997 Seedling recruitment in semi-natural pastures: the effects of disturbance, seed size, phenology and seed bank. *Nordic J. Bot.* **17**, 469–482.

Goodman, L. A. 1969 The analysis of population growth when birth and death rates depend upon several factors. *Biometrics* **25**, 659–681.

Greig-Smith, J. & Sagar, G. R. 1981 Biological causes of local rarity in *Carlina vulgaris*. In *The biological aspects of rare plant conservation* (ed. H. Synge), pp. 389–400. London: Wiley.

Gross, K. L. 1981 Predictions of fate from rosette size in four 'biennial' plant species: *Verbascum thapsus, Oenothera biennis, Daucus carota,* and *Tragopogon dubius. Oecologia* **48**, 209–213.

Kachi, N. & Hirose, T. 1985 Population-dynamics of *Oenothera glazioviana* in a sand-dune system with special reference to the adaptive significance of size-dependent reproduction. *J. Ecol.* **73**, 887–901.

Karlsson, P. S. & Jacobson, A. 2001 Onset of reproduction in *Rhododendron lapponicum* shoots: the effect of shoot size, age, and nutrient status at two subarctic sites. *Oikos* **94**, 279–286.

Klinkhamer, P. G. L., de Jong, T. J. & Meelis, E. 1987 Delay of flowering in the biennial *Cirsium vulgare*: size effects and devernalization. *Oikos* **49**, 303–308.

Klinkhamer, P. G. L., de Jong, T. J. & Meelis, E. 1991 The control of flowering in the monocarpic perennial *Carlina vulgaris. Oikos* **61**, 88–95.

Klinkhamer, P. G. L., de Jong, T. J. & de Heiden, J. L. H. 1996 An 8-year study of population-dynamics and life-history variation of the biennial *Carlina vulgaris. Oikos* **75**, 259–268.

Krasnosel'skij, M. A., Lifshits, J. A. & Sobolev, A. V. 1989 *Positive linear systems: the method of positive operators.* Berlin: Helderman Verlag.

Law, R. 1983 A model for the dynamics of a plant-population containing individuals classified by age and size. *Ecology* **64**, 224–230.

Law, R. & Edley, M. T. 1990 Transient dynamics of populations with age-dependent and size-dependent vital-rates. *Ecology* **71**, 1863–1870.

Lei, S. A. 1999 Age, size and water status of *Acacia gregii* influencing the infection and reproductive success of *Phoradendron californicum. Am. Midl. Nat.* **141**, 358–365.

Lofgren, P., Eriksson, O. & Lehtila, K. 2000 Population dynamics and the effect of disturbance in the monocarpic herb *Carlina vulgaris* (Asteraceae). *Annls Bot. Fenn.* **37**, 183–192.

McCullagh, P. & Nelder, J. A. 1989 *Generalized linear models.* Monographs on statistics and applied probability. London: Chapman & Hall.

McGraw, J. B. 1989 Effects of age and size on life histories and population growth of *Rhododendron maximum* shoots. *Am. J. Bot.* **76**, 113–123.

Metcalf, J. C., Rose, K. E. & Rees, M. 2003 Gambling on an uncertain existence: evolutionary demography of monocarpic perennials. *Trends Ecol. Evol.* (In the press.)

Metz, J. A. J., Nisbet, R. M. & Geritz, S. A. H. 1992 How should we define fitness for general ecological scenarios. *Trends Ecol. Evol.* **7**, 198–202.

Mylius, S. D. & Diekmann, O. 1995 On evolutionarily stable life-histories, optimization and the need to be specific about density-dependence. *Oikos* **74**, 218–224.

Rand, D. A., Wilson, H. B. & McGlade, J. M. 1994 Dynamics and evolution—evolutionarily stable attractors, invasion

exponents and phenotype dynamics. *Phil. Trans. R. Soc. Lond.* B **343**, 261–283.

Rees, M. & Long, M. J. 1993 The analysis and interpretation of seedling recruitment curves. *Am. Nat.* **141**, 233–262.

Rees, M. & Rose, K. E. 2002 Evolution of flowering strategies in *Oenothera glazioviana*: an integral projection model approach. *Proc. R. Soc. Lond.* B **269**, 1509–1515. (DOI 10.1098/rspb.2002.2037.)

Rees, M., Sheppard, A., Briese, D. & Mangel, M. 1999 Evolution of size-dependent flowering in *Onopordum illyricim*: a quantitative assessment of the role of stochastic selection pressures. *Am. Nat.* **154**, 628–651.

Rees, M., Mangel, M., Turnbull, L. A., Sheppard, A. & Briese, D. 2000 The effects of heterogeneity on dispersal and colonisation in plants. In *Ecological consequences of environmental heterogeneity* (ed. M. J. Hutchings, E. A. John & A. J. A. Stewart), pp. 237–265. Oxford: Blackwell Scientific.

Rose, K. E., Rees, M. & Grubb, P. J. 2002 Evolution in the real world: stochastic variation and the determinants of fitness in *Carlina vulgaris. Evolution* **56**, 1416–1430.

Simons, A. M. & Johnston, M. O. 2000 Plasticity and the genetics of reproductive behaviour in the monocarpic perennial, *Lobelia inflata* (Indian tobacco). *Heredity* **85**, 356–365.

Sletvold, N. 2002 Effects of plant size on reproductive output and offspring performance in the facultative biennial *Digitalis purpurea. J. Ecol.* **90**, 958–966.

van Groenendael, J. M. & Slim, P. 1988 The contrasting dynamics of two populations of *Plantago lanceolata* classified by age and size. *J. Ecol.* **76**, 585–599.

Venables, W. N. & Ripley, B. D. 1997 *Modern applied statistics with S-PLUS.* New York: Springer.

Weiner, J., Martinez, S., MullerScharer, H., Stoll, P. & Schmid, B. 1997 How important are environmental maternal effects in plants? A study with *Centaurea maculosa. J. Ecol.* **85**, 133–142.

Werner, P. A. 1975 Predictions of fate from rosette size in teasel (*Dipsacus fullonum* L.). *Oecologia* **20**, 197–201.

Wesselingh, R. A. & de Jong, T. J. 1995 Bidirectional selection on threshold size for flowering in *Cynoglossum officinale* (hounds tongue). *Heredity* **74**, 415–424.

Wesselingh, R. A. & Klinkhamer, P. G. L. 1996 Threshold size for vernalization in *Senecio jacobaea*: genetic variation and response to artificial selection. *Funct. Ecol.* **10**, 281–288.

Wesselingh, R. A., Klinkhamer, P. G. L., de Jong, T. J. & Boorman, L. A. 1997 Threshold size for flowering in different habitats: effects of size-dependent growth and survival. *Ecology* **78**, 2118–2132.

Wood, S. N. 2001 Partially specified ecological models. *Ecol. Monogr.* **71**, 1–25.

Wright, S. 1931 Evolution in Mendelian populations. *Genetics* **16**, 97–159.